Editors' Suggestion

Bath-mediated interactions between driven tracers in dense single files

Alexis Poncet,[1] Olivier Bénichou,[1] Vincent Démery,[2,3] and Gleb Oshanin[1]

[1]*LPTMC, CNRS and Sorbonne Université, 4 Place Jussieu, 75005 Paris, France*

[2]*Gulliver, UMR CNRS 7083, ESPCI Paris, PSL Research University, 10 rue Vauquelin, 75005 Paris, France*

[3]*Univ Lyon, ENS de Lyon, Univ Claude Bernard, CNRS, Laboratoire de Physique, 69342 Lyon, France*

(Received 15 July 2019; published 8 November 2019)

Single-file transport, where particles cannot bypass each other, has been observed in various experimental setups. In such systems, the behavior of a tracer particle (TP) is subdiffusive, which originates from strong correlations between particles. These correlations are especially marked when the TP is driven and leads to inhomogeneous density profiles. Determining the impact of this inhomogeneity when several TPs are driven in the system is a key question, related to the general issue of bath-mediated interactions, which are known to induce collective motion and lead to the formation of clusters or lanes in a variety of systems. Quantifying this collective behavior, the emerging interactions, and their dependence on the amplitude of forces driving the TPs remains a challenging but largely unresolved issue. Here, considering dense single-file systems, we analytically determine the entire dynamics of the correlations and reveal out-of-equilibrium cooperativity and competition effects between driven TPs.

DOI: 10.1103/PhysRevResearch.1.033089

The motion of particles in narrow channels in which particles cannot bypass each other is known as single-file diffusion. Such systems have been studied in various experimental setups with zeolites [1,2], microchannels [3,4], nanochannels [5], and simulations of carbon nanotubes [6]. Key features, on the theoretical side, involve the existence of a subdiffusive scaling for the mean position of a given particle [7,8] and strong correlations between particles [9].

The basic phenomenology of the single-file transport is well captured by the symmetric exclusion process (SEP). In this paradigmatic model of crowded equilibrium systems, particles perform symmetric random walks on a one-dimensional lattice with the constraint of at most a single occupancy of each lattice site. Different facets of the SEP have been scrutinized (see Refs. [8,10–15]), including several important extensions to out-of-equilibrium situations. In particular, the mean displacement [16], as well as all higher-order cumulants [17], of an unbiased tagged particle (TP) placed initially at the shock point of a steplike density profile has been determined. Moreover, for a SEP with a *single* biased TP (due to either an energy consumption or an external force), the mean displacement of the latter [18,19] and the higher-order cumulants in the dense limit [20] have been calculated and shown to grow sublinearly as $\sqrt{t}$. Here the particles accumulate in front of the TP and are depleted behind it, which results in an inhomogeneous, nonstationary spatial distribution of particles.

A general open question concerns situations when *several* biased TPs are introduced in an otherwise quiescent medium of bath particles. The TPs are then expected to entrain the bath particles in a directional motion, which brings the system out of equilibrium and gives rise to effective bath-mediated interactions (BMIs) between the TPs. Such BMIs potentially lead to self-organization, as observed in systems as diverse as colloidal solutions [21–30], nearly critical fluid mixtures [31], dusty complex plasmas [32], and pedestrian counterflows [33].

Quantifying the emerging interactions between biased TPs and the ensuing collective behavior is thus a key issue which however remains largely unresolved. Here, modeling a host medium as a dense SEP, we analytically determine the temporal evolution of all correlation functions, reveal intrinsically out-of-equilibrium cooperativity and competition effects between multiple TPs, and quantify BMIs.

The quiescent host medium is modeled as a SEP which involves a high density ρ ($\rho \to 1$) of hard-core bath particles performing *symmetric* random walks (with unit jump rate) on a one-dimensional lattice. We then tag N particles at initial positions X_j^0 (see Fig. 1). These TPs are biased: The jth TP jumps to the left (right) with probability $(1 - s_j)/2$ $[(1 + s_j)/2]$. The bias $s_j \in (-1, 1)$ may be due either to an "activity" of the particle or to an external force f_j, in which case one has the detailed balance condition $e^{\beta f_j} = \frac{1+s_j}{1-s_j}$, with β the reciprocal temperature.

We aim at determining the correlations between the TPs, embodied in the so-called cumulant-generating function $\psi(\mathbf{k}, t) \equiv \ln\langle e^{i\mathbf{k}\cdot\mathbf{Y}(t)}\rangle$, where $\mathbf{k} = (k_1, \ldots, k_N)$ and $\mathbf{Y} = (Y_1, \ldots, Y_N)$, with $Y_j(t) = X_j(t) - X_j^0$ the displacement of the jth TP. The cumulants are denoted by $\langle\bullet\rangle_c$ and defined by the expansion

$$\psi(\mathbf{k}, t) = \sum_{p_1,\ldots,p_N=0}^{\infty} \frac{(ik_1)^{p_1}\cdots(ik_N)^{p_N}}{(p_1 + \cdots + p_N)!}\left\langle Y_1^{p_1}\cdots Y_N^{p_N}\right\rangle_c. \quad (1)$$

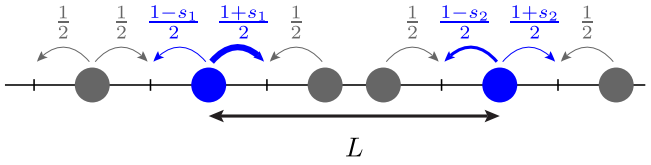

FIG. 1. System with two tagged particles. All particles perform random walks with unit jump rate, constrained by hard-core exclusion. Bath particles jump to the left or right with probability 1/2. The TPs jump with probabilities $(1 \pm s_j)/2$. L is the initial distance between TPs.

In densely populated single files ($\rho \to 1$), the dynamics of the system can be reformulated in terms of independent vacancies. In essence, this amounts to neglecting events where two vacancies interact simultaneously with any TP [20,34]. Our approach is based first on considering an auxiliary problem involving a single vacancy, initially at position U. By counting all the interactions of this vacancy with the TPs, we determine the probability $p_U(\mathbf{Y}, t)$ that the TPs have displacements $\mathbf{Y}$ at time t. Then, for a density of vacancies $\rho_0 = 1 - \rho \to 0$, the cumulant-generating function reads [35]

$$\lim_{\rho_0 \to 0} \frac{\psi(\mathbf{k}, t)}{\rho_0} = \sum_{U \notin \{X_i^0\}} [\tilde{p}_U(\mathbf{k}, t) - 1], \tag{2}$$

where $\tilde{p}_U(\mathbf{k}, t)$ is the Fourier transform of $p_U(\mathbf{Y}, t)$ and can be expressed in terms of first-passage quantities of simple random walks with or without absorbing sites [36]. Analysis of the explicit expression of the cumulant-generating function for densely populated single files [35] allows us to draw a number of important conclusions, which we present below.

Bath-mediated binding. As expected, at short times, the TPs move independently subject to their own biases. Our first finding is that, at long times and at high particle density, they are moving as a single TP. More precisely, in the long-time limit the N-TP cumulants are given by $\langle Y_1 \cdots Y_N^{q_N} \rangle_c = \langle Z^{q_1 + \cdots + q_N} \rangle_c$ for positive integer q_j, where $Z = \sum_{j=1}^N Y_j/N$ is the displacement of the center of mass. At high density, even and odd cumulants of Z satisfy

$$\frac{\langle Z(t)^{2n} \rangle_c}{\rho_0} = \frac{\langle Z(t)^{2n+1} \rangle_c}{\rho_0 S} = \sqrt{\frac{2t}{\pi}}, \tag{3}$$

where $S = \tanh(\beta F/2)$ is the effective bias, $F = \sum_{j=1}^N f_j$ is the effective force, and the ratio $\langle \bullet \rangle / \rho_0$ is understood as the limit $\rho_0 \to 0$. Equation (3) implies in particular that for any number of TPs and arbitrary forces $\langle Y_j \rangle = \langle Z \rangle$, meaning that at long times all the TPs move like their center of mass with an effective force F (in agreement with the hydrodynamic analysis of Ref. [37]).

In the following, we determine the full dynamics of the correlations between TPs and focus for simplicity on the case of two TPs.

Bath-mediated entrainment. We examine the case of a single biased TP ($s_2 \neq 0$) followed by an unbiased TP ($s_1 = 0$), initially separated by a distance L [see Fig. 2(a)], which allows us to quantify the perturbation induced by a biased tracer in a quiescent medium. While the behavior of $\langle Y_2 \rangle$ is known [20], we unveil an interesting scaling behavior of $\langle Y_1 \rangle$

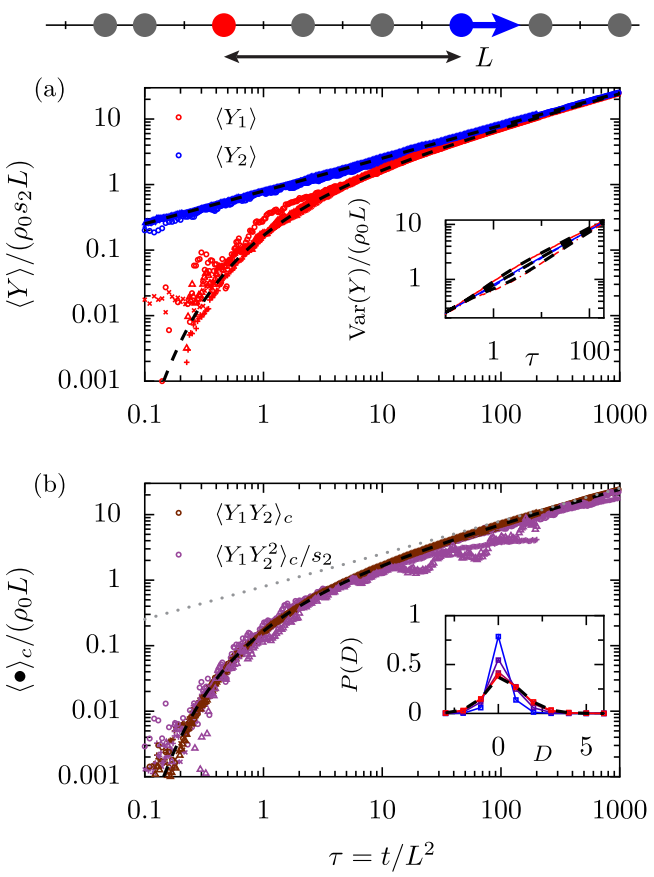

FIG. 2. Entrainment of the bath particles by a biased TP for $\rho_0 = 10^{-2}$. Only the right TP is biased. (a) Evolution of the mean displacements, with different symbols corresponding to $L = 10, 50$ and $s_2 = -0.2, 0.8$. The black lines are the predictions from Eq. (4). (b) Cumulants $\langle Y_1 Y_2 \rangle_c$ and $\langle Y_1 Y_2^2 \rangle_c / s_2$ for the same set of parameters as in (a). The black line corresponds to Eq. (6). The inset of (a) shows variances for $L = 10$, $s_2 = 0.8$ (solid lines) and $L = 10$, $s_2 = -0.8$ (dashed lines). Predictions are in black [35]. The inset of (b) shows the law of the variation of distance $D = Y_2 - Y_1$ at times $10, 10^2, 10^3, 10^4$ (blue to red) for $L = 10$, $s = 0.8$, and $\rho_0 = 0.05$. The squares are the numerical results, the colored lines are the theoretical predictions, and the black line is the asymptotic prediction [35].

beyond the long-time regime. Indeed, in the limit $t \to \infty$ with t/L^2 constant, one finds

$$\frac{\langle Y_2(t) \rangle}{\rho_0} = s_2 \sqrt{\frac{2t}{\pi}}, \quad \frac{\langle Y_1(t) \rangle}{\rho_0} = s_2 \sqrt{\frac{2t}{\pi}} g\left(\frac{L}{\sqrt{2t}} \right), \tag{4}$$

$$g(u) = e^{-u^2} - \sqrt{\pi}\, u \operatorname{erfc}(u). \tag{5}$$

This provides the dynamics of the entrainment of TP1 by TP2, which admits a typical time scale L^2 and leads to the final bound state discussed above (see Fig. 2).

The evolution towards the final regime can further be quantified by the dynamics of the two-TP even (odd) cumulants $\kappa^e = \langle Y_1^p Y_2^q \rangle_c$ ($\kappa^o = \langle Y_1^p Y_2^q \rangle_c$) with $p + q$ even (odd), $p, q \geqslant 1$. They obey

$$\frac{\kappa^e}{\rho_0} = \frac{\kappa^o}{\rho_0 s_2} = \sqrt{\frac{2t}{\pi}} g\left(\frac{L}{\sqrt{2t}} \right). \tag{6}$$

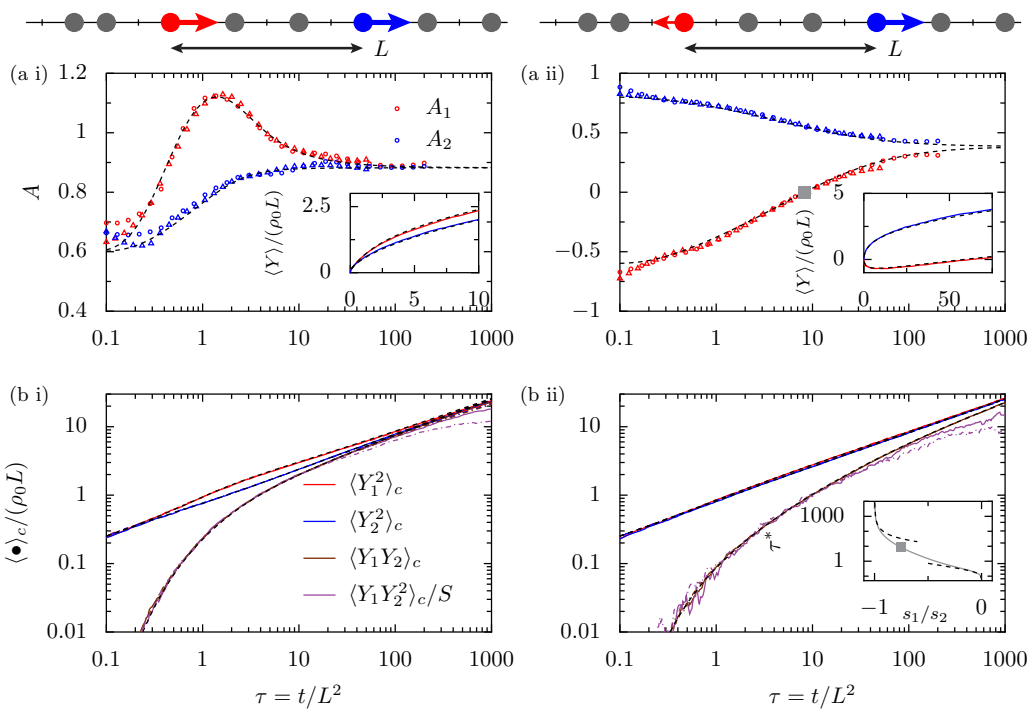

FIG. 3. Cooperativity and competition ($\rho_0 = 10^{-2}$). (a i) and (b i) The two TPs have identical biases $s_1 = s_2 = 0.8$. (a ii) and (b ii) The biases are in opposite directions $s_1 = -0.6$ and $s_2 = 0.8$. The rescaled velocities A are plotted in (a i) and (a ii) with the displacements in the inset; two initial distances are plotted: $L = 50$ and 200. At short times, the rescaled velocities are s_1 and s_2; at long times they are both equal to S. The variances and some cumulants are plotted in (b i) and (b ii) (initial distances $L = 10$ and 20). In the case in (a ii) and (b ii), the velocity of the first TP changes sign at rescaled time $\tau^* = t^*/L^2$ [gray square in (a ii)]. The prediction τ^* is plotted as a function of s_1/s_2 for $s_2 = 0.8$. The dashed lines are the asymptotic behaviors from Eq. (12); the gray square corresponds to the one in (a ii).

Several comments are in order. (i) Equations (4) and (6) are similar to the expressions found for the random average process [38,39], which points towards their universality. (ii) The same scaling function g is involved in the expressions of $\langle Y_1(t)\rangle$ and $\langle Y_1Y_2(t)\rangle_c$ [Eqs. (4) and (6)]. This leads to the generalized fluctuation-dissipation relation

$$\lim_{f_2\to 0}\frac{2}{\beta}\frac{\langle Y_1(f_1=0,f_2)\rangle}{f_2} = \langle Y_1Y_2\rangle_c(f_1=f_2=0). \quad (7)$$

Note that this relation holds in the opposite limit of a dilute ($\rho \to 0$) SEP [40]. (iii) Our approach provides the time dependence of all cumulants of individual particles and the law of the distance between TPs (insets of Fig. 2 and [35]). The time, initial distance between TPs, and driving force dependences from numerical simulations are unambiguously captured by our theoretical expressions (Fig. 2).

Bath-mediated cooperatively and competition. We now turn to the general case in which both TPs are biased [see Fig. 3(a)]. The dynamics of effective interactions between TPs at the level of averages is conveniently analyzed by introducing the rescaled instantaneous velocities

$$A_j(t) = \frac{\sqrt{2\pi t}}{\rho_0}\frac{d\langle Y_j\rangle}{dt}, \quad (8)$$

which satisfy $A_j(t) = s_j$ at short times and $A_j(t) = S = \frac{s_1+s_2}{1+s_1s_2}$ at long times. The full time dependence is found [35] to be given by $A_1 = H_{s_1,s_2(1+s_1),-s_1s_2}(L/\sqrt{2t})$ and $A_2 = H_{s_2,s_1(1-s_2),s_1s_2}(L/\sqrt{2t})$, with

$$H_{\beta_0,\beta_1,\beta_2}(u) = \sum_{n=0}^{\infty}(-s_1s_2)^n\sum_{m=0}^{2}\beta_m e^{-[(2n+m)u]^2}, \quad (9)$$

while higher-order cumulants follow

$$\frac{\kappa^e}{\rho_0} = \frac{\kappa^o}{\rho_0 S} = \sqrt{\frac{2t}{\pi}}G_{s_1s_2}\left(\frac{L}{\sqrt{2t}}\right), \quad (10)$$

$$G_\sigma(u) = (1+\sigma)\sum_{n=0}^{\infty}(-\sigma)^n g([2n+1]u). \quad (11)$$

These results fully quantify the dynamics of the BMIs between two biased TPs and reveal striking behaviors. (i) In the case of same sign biases, the TPs cooperate [37] [Figs. 3(a i) and 3(b i)]. At long times a pair of biased TPs moves faster than a single TP, in agreement with the asymptotic result (3). Note that such an accelerated dynamics has been numerically observed in two-dimensional systems [22,24]. At intermediate times, we unveil an overshoot of the rescaled velocity of the trailing TP. (ii) When the biases act in opposite directions (say, $0 < -s_1 < s_2$), each TP starts to move in the direction of its own force and eventually both TPs move in the direction of the largest force [Figs. 3(a i) and 3(b i)]. This competing stage can be quantified from Eq. (9) by determining the U-turn time t^* at which the velocity of TP1 changes its sign. This time t^*

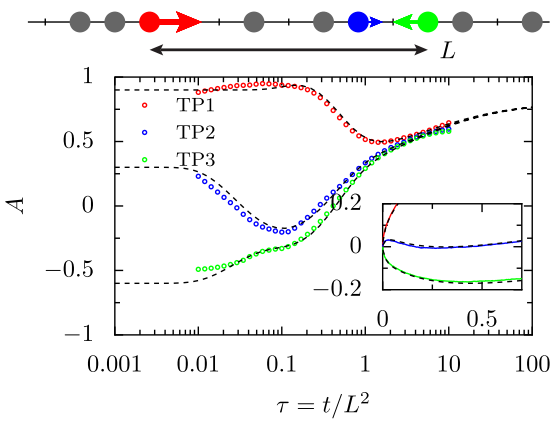

FIG. 4. Rescaled velocity of three TPs for biases $s_1 = 0.9$, $s_2 = 0.3$, and $s_3 = -0.6$, total distance $L = X_3^0 - X_1^0 = 60$ with $X_2^0 - X_1^0 = 45$, and $\rho_0 = 10^{-2}$. The colored circles correspond to the numerical simulations while the dashed lines are the theoretical predictions [35]. The inset shows the average displacements of the TPs in linear rescaled time. The behavior of the second TP displays several regimes: It first moves to the right, then under the influence of the third TP it goes to the left, and finally the first TP pushes it back to the right. Note that this complex dynamics is captured by our theoretical approach.

vanishes when s_1 is small and diverges when s_1 is close to $-s_2$ according to the scaling laws

$$\frac{t^*}{L^2} \underset{s_1\to 0}{\sim} \frac{1}{2\ln(-s_2/s_1)}, \quad \frac{t^*}{L^2} \underset{s_1\to -s_2}{\sim} \frac{\gamma}{1+s_1/s_2}, \tag{12}$$

with $\gamma = 2(1+s_2)^2/(1-s_2)$. Figure 3 shows excellent quantitative agreement between the analytical predictions and the numerical simulations.

Our approach can be extended to determine the dynamics of correlations in the case of an arbitrary number of driven TPs. Cooperativity and competition involve a complex cascade of timescales associated with the initial distances between TPs, fully captured by our approach, as exemplified in the case of three TPs in Fig. 4 and [35].

Bath-mediated interactions. The BMIs between two bound biased TPs can be further analyzed by associating the probability distribution of the variation of distance $D = Y_2 - Y_1$ with an effective potential $U(D)$ via $P(D) = \exp[-\beta U(D)]$ [41]. For identical forces ($f_1 = f_2 = f$) and D sufficiently close to its average value, the two TPs are effectively bound by a harmonic potential

$$U(D) \sim \frac{\kappa}{2}(D - \langle D\rangle)^2, \quad \frac{\langle D\rangle}{\rho_0 L} = \left(\frac{1}{\cosh(\beta f)} - 1\right), \tag{13}$$

where the constant κ is explicitly given by

$$\kappa = \frac{\cosh(\beta f)}{\beta\rho_0 L[1+\cosh(\beta f)]}. \tag{14}$$

In the regime $D \gg \langle D\rangle$, the potential displays a weaker dependence on the distance $U(D) \sim D(\ln D + \nu)/\beta$ (see [35] for the value of ν). We remark that this qualitative change of regimes has been observed in two dimensions in numerical simulations of two biased TPs in a quiescent colloidal bath [24].

Altogether, we determined the full dynamics of correlation functions in a paradigmatic model of nonequilibrium statistical physics and entirely characterized the corresponding bath-mediated interactions.

[1] V. Gupta, S. S. Nivarthi, A. V. McCormick, and H. T. Davis, Chem. Phys. Lett. **247**, 596 (1995).
[2] K. Hahn, J. Kärger, and V. Kukla, Phys. Rev. Lett. **76**, 2762 (1996).
[3] Q.-H. Wei, C. Bechinger, and P. Leiderer, Science **287**, 625 (2000).
[4] B. Lin, M. Meron, B. Cui, S. A. Rice, and H. Diamant, Phys. Rev. Lett. **94**, 216001 (2005).
[5] T. Meersmann, J. W. Logan, R. Simonutti, S. Caldarelli, A. Comotti, P. Sozzani, L. G. Kaiser, and A. Pines, J. Phys. Chem. A **104**, 11665 (2000).
[6] A. Berezhkovskii and G. Hummer, Phys. Rev. Lett. **89**, 064503 (2002).
[7] T. E. Harris, J. Appl. Probab. **2**, 323 (1965).
[8] R. Arratia, Ann. Probab. **11**, 362 (1983).
[9] A. Poncet, O. Bénichou, V. Démery, and G. Oshanin, Phys. Rev. E **97**, 062119 (2018).
[10] D. G. Levitt, Phys. Rev. A **8**, 3050 (1973).
[11] P. A. Fedders, Phys. Rev. B **17**, 40 (1978).
[12] S. Alexander and P. Pincus, Phys. Rev. B **18**, 2011 (1978).
[13] L. Lizana, T. Ambjörnsson, A. Taloni, E. Barkai, and M. A. Lomholt, Phys. Rev. E **81**, 051118 (2010).
[14] A. Taloni and M. A. Lomholt, Phys. Rev. E **78**, 051116 (2008).
[15] G. Gradenigo, A. Puglisi, A. Sarracino, A. Vulpiani, and D. Villamaina, Phys. Scr. **86**, 058516 (2012).
[16] G. Oshanin, O. Bénichou, S. F. Burlatsky, and M. Moreau, in *Instabilities and Nonequilibrium Structures IX*, edited by O. Descalzi, J. Martínez, and S. Rica (Springer, Dordrecht, 2004), Vol. 9, p. 33.
[17] T. Imamura, K. Mallick, and T. Sasamoto, Phys. Rev. Lett. **118**, 160601 (2017).
[18] S. F. Burlatsky, G. Oshanin, M. Moreau, and W. P. Reinhardt, Phys. Rev. E **54**, 3165 (1996).
[19] C. Landim, S. Olla, and S. B. Volchan, Commun. Math. Phys. **192**, 287 (1998).
[20] P. Illien, O. Bénichou, C. Mejía-Monasterio, G. Oshanin, and R. Voituriez, Phys. Rev. Lett. **111**, 038102 (2013).
[21] C. Reichhardt and C. J. O. Reichhardt, Phys. Rev. E **74**, 011403 (2006).
[22] C. Mejía-Monasterio and G. Oshanin, Soft Matter **7**, 993 (2011).
[23] I. Ladadwa and A. Heuer, Phys. Rev. E **87**, 012302 (2013).
[24] O. A. Vasilyev, O. Bénichou, C. Mejía-Monasterio, E. R. Weeks, and G. Oshanin, Soft Matter **13**, 7617 (2017).

[25] M. E. Leunissen, C. G. Christova, A.-P. Hynninen, C. P. Royall, A. I. Campbell, A. Imhof, M. Dijkstra, R. van Roij, and A. van Blaaderen, Nature (London) **437**, 235 (2005).
[26] M. Rex and H. Löwen, Eur. Phys. J. E **26**, 143 (2008).
[27] T. Vissers, A. Wysocki, M. Rex, H. Löwen, C. P. Royall, A. Imhof, and A. van Blaaderen, Soft Matter **7**, 2352 (2011).
[28] T. Glanz and H. Löwen, J. Phys.: Condens. Matter **24**, 464114 (2012).
[29] A. Poncet, O. Bénichou, V. Démery, and G. Oshanin, Phys. Rev. Lett. **118**, 118002 (2017).
[30] N. Bain and D. Bartolo, Nat. Commun. **8**, 15969 (2017).
[31] A. Furukawa, A. Gambassi, S. Dietrich, and H. Tanaka, Phys. Rev. Lett. **111**, 055701 (2013).
[32] K. R. Sütterlin, A. Wysocki, A. V. Ivlev, C. Räth, H. M. Thomas, M. Rubin-Zuzic, W. J. Goedheer, V. E. Fortov, A. M. Lipaev, V. I. Molotkov *et al.*, Phys. Rev. Lett. **102**, 085003 (2009).
[33] D. Helbing, Rev. Mod. Phys. **73**, 1067 (2001).
[34] M. J. A. M. Brummelhuis and H. J. Hilhorst, J. Stat. Phys. **53**, 249 (1988).
[35] See Supplemental Material at http://link.aps.org/supplemental/10.1103/PhysRevResearch.1.033089 for details of the numerical simulations and detailed calculations.
[36] B. D. Hughes, *Random Walks and Random Environments* (Oxford University Press, Oxford, 1995), Vol. 1.
[37] O. Bénichou, V. Démery, and A. Poncet, Phys. Rev. Lett. **120**, 070601 (2018).
[38] R. Rajesh and S. N. Majumdar, Phys. Rev. E **64**, 036103 (2001).
[39] J. Cividini, A. Kundu, S. N. Majumdar, and D. Mukamel, J. Stat. Mech. (2016) 053212.
[40] T. Ooshida and M. Otsuki, J. Phys.: Condens. Matter **30**, 374001 (2018).
[41] A. Y. Grosberg and J.-F. Joanny, Phys. Rev. E **92**, 032118 (2015).